

Blurred image recognition by legendre moment invariants

Hui Zhang^{1,2}, Huazhong Shu^{1,2*}, Guo-Niu Han³, Gouenou Coatrieux⁴, Limin Luo^{1,2}, Jean-Louis Coatrieux^{2,5}

¹ LIST, Laboratory of Image Science and Technology SouthEast University, Si Pai Lou 2, Nanjing, 210096, CN

² CRIBS, Centre de Recherche en Information Biomédicale sino-français INSERM : Laboratoire International Associé, Université de Rennes I, SouthEast University, Nankin, CN

³ IRMA, Institut de Recherche Mathématique Avancée CNRS : UMR7501, Université Louis Pasteur - Strasbourg I, 7 rue René-Descartes, 67084 Strasbourg Cedex, France, FR

⁴ LATIM - Laboratoire de Traitement de l'Information Médicale INSERM : U650, Université de Bretagne Occidentale - Brest, Institut Télécom, Télécom Bretagne, Université européenne de Bretagne, CHU Brest, Hopital Morvan, 5 Avenue Foch, 29609 Brest Cedex, FR

⁵ LTSI, Laboratoire Traitement du Signal et de l'Image INSERM : U642, Université de Rennes I, Campus de Beaulieu, 263 Avenue du Général Leclerc - CS 74205 - 35042 Rennes Cedex, FR

* Correspondence should be addressed to: Huazhong Shu <shu.list@seu.edu.cn >

Abstract

Processing blurred images is a key problem in many image applications. Existing methods to obtain blur invariants which are invariant with respect to centrally symmetric blur are based on geometric moments or complex moments. In this paper, we propose a new method to construct a set of blur invariants using the orthogonal Legendre moments. Some important properties of Legendre moments for the blurred image are presented and proved. The performance of the proposed descriptors is evaluated with various point-spread functions and different image noises. The comparison of the present approach with previous methods in terms of pattern recognition accuracy is also provided. The experimental results show that the proposed descriptors are more robust to noise and have better discriminative power than the methods based on geometric or complex moments.

Author Keywords Blur Invariants ; Blurred Image ; Data mining ; Gaussian noise ; Imaging ; Legendre Moments ; Pattern Recognition ; Pixel ; Robustness ; Symmetric Blur.

Introduction

Image processing is a very active area that has impacts in many domains from remote sensing, robotics, traffic surveillance to medicine. Automatic target recognition and tracking, character recognition, three-dimensional (3-D) scene analysis and reconstruction are only a few objectives to deal with. Since the real sensing systems are usually imperfect and the environmental conditions are changing over time, the acquired images often provide a degraded version of the true scene. An important class of degradations we are faced with in practice is image blurring, which can be caused by diffraction, lens aberration, wrong focus, and atmospheric turbulence. In pattern recognition, two options have been widely explored either through a two steps approach by restoring the image and then applying recognition methods, or by designing a direct one-step solution, free of blurring effects. In the former case, the point spread function (PSF), most often unknown in real applications, should be estimated [1 –5]. In the latter case, finding a set of invariants that are not affected by blurring is the key problem and the subject of this paper.

The pioneering work in this field was performed by Flusser and Suk [6] who derived invariants to convolution with an arbitrary centrosymmetric PSF. These invariants have been successfully used in template matching of satellite images [6], in pattern recognition [7] –[10], in blurred digit and character recognition [11], [12], in normalizing blurred images into canonical forms [13], [14], and in focus/defocus quantitative measurement [15]. More recently, Flusser and Zitova introduced the combined blur-rotation invariants [16] and reported their successful application to satellite image registration [17] and camera motion estimation [18]. Suk and Flusser further proposed a set of combined invariants which are invariant to affine transform and to blur [19]. The extension of blur invariants to N-dimensions has also been investigated [20], [21]. All the existing methods to derive the blur invariants are based on geometric moments or complex moments. However, both geometric moments and complex moments contain redundant information and are sensitive to noise especially when high-order moments are concerned. This is due to the fact that the kernel polynomials are not orthogonal.

Teague has suggested the use of orthogonal moments to recover the image from moments [22]. It was shown that the orthogonal moments are better than other types of moments in terms of information redundancy, and are more robust to noise [23]. As noted by Teh and Chin [23], the moment invariants are considered reliable features in pattern recognition if they are insensitive to the presence of image noise. Consequently, it could be expected that the use of orthogonal moments in the construction of blur invariant provides better recognition results. To the authors' knowledge, no orthogonal moments have been used to construct the blur invariants.

In this paper, we propose a new method to derive a set of blur invariants based on orthogonal Legendre moments (for a recent survey on moments, refer to [24]–[27]). The organization of this paper is as follows: in Section 2, we review the theory of blur invariants of geometric moments and the definition of Legendre moments. In Section 3, we establish a relationship between the Legendre moments of the blurred image and those of the original image and the PSF. Based on this relationship, a set of blur invariants using Legendre moments is provided. The experimental results for evaluating the performance of the proposed descriptors are given in Section 4. Finally, some concluding remarks are provided.

BLUR INVARIANTS AND LEGENDRE MOMENTS

This section first reviews the theory of blur invariants of geometric moments proposed by Flusser and Suk [6], [7], and then presents some basic definitions of Legendre moments.

Blur invariants of geometric moments

The two-dimensional (2-D) geometric moment of order $(p+q)$, with image intensity function $f(x, y)$, is defined as

$$m_{pq}^{(f)} = \int_{-1}^1 \int_{-1}^1 x^p y^q f(x, y) dx dy,$$

where, without loss of generality, we assume that the image function $f(x, y)$ is defined on the square $[-1, 1] \times [-1, 1]$.

The corresponding central moment of image $f(x, y)$ is defined as

$$\mu_{pq}^{(f)} = \int_{-1}^1 \int_{-1}^1 (x - x_0^{(f)})^p (y - y_0^{(f)})^q f(x, y) dx dy,$$

with the coordinates $(x_0^{(f)}, y_0^{(f)})$ denoting the centroid of $f(x, y)$

$$x_0^{(f)} = \frac{m_{10}^{(f)}}{m_{00}^{(f)}}, \quad y_0^{(f)} = \frac{m_{01}^{(f)}}{m_{00}^{(f)}}.$$

Let $g(x, y)$ be a blurred version of the original image $f(x, y)$. The blurring is classically described by the convolution

$$g(x, y) = (f * h)(x, y)$$

where $h(x, y)$ is the PSF of the imaging system, and $*$ denotes linear convolution.

In this paper, we assume that the PSF, $h(x, y)$, is a centrally symmetric image function and the imaging system is energy-preserving, that is,

$$\begin{aligned} h(x, y) &= h(-x, -y) \\ \int_{-1}^1 \int_{-1}^1 h(x, y) dx dy &= 1. \end{aligned}$$

As noted by Flusser [7], the assumption of centrally symmetry is not a significant limitation of practical utilization of the method. Most real sensors and imaging systems have PSFs with certain degrees of symmetry. In many cases they have even higher symmetry than central, such as axial or radial symmetry. Thus, the central symmetry assumption is general enough to describe almost all practical situations.

Lemma 1

The centroid of the blurred image $g(x, y)$ is related to the centroid of the original image $f(x, y)$ and that of the PSF $h(x, y)$ as

$$\begin{aligned} x_0^{(g)} &= x_0^{(f)} + x_0^{(h)}, \\ y_0^{(g)} &= y_0^{(f)} + y_0^{(h)}. \end{aligned}$$

In particular, if $h(x, y)$ is centrally symmetric, then $x_0^{(h)} = y_0^{(h)} = 0$. In such a case, we have $x_0^{(g)} = x_0^{(f)}$, $y_0^{(g)} = y_0^{(f)}$.

The proof of Lemma 1 can be found in [9].

Legendre moments

The 2-D (p+q)th order Legendre moment of image function $f(x, y)$ is defined as [28]

$$L_{pq}^{(f)} = \int_{-1}^1 \int_{-1}^1 P_p(x) P_q(y) f(x, y) dx dy, \quad p, q = 0, 1, 2, \dots,$$

where $P_p(x)$ is the p th-order orthonormal Legendre polynomials given by

$$P_p(x) = \sum_{k=0}^p c_{p,k} x^k,$$

with

$$c_{p,k} = \begin{cases} \sqrt{\frac{2p+1}{2}} \frac{(-1)^{\frac{p-k}{2}} (p+k)!}{2^p (\frac{p-k}{2})! (\frac{p+k}{2})!}, & p-k = \text{even} \\ 0 & p-k = \text{odd} \end{cases}$$

The corresponding central moments are defined as

$$L_{pq}^{(f)} = \int_{-1}^1 \int_{-1}^1 P_p(x - x_0^{(f)}) P_q(y - y_0^{(f)}) f(x, y) dx dy,$$

where the coordinates $(x_0^{(f)}, y_0^{(f)})$ are defined in (3).

Method

In this section, we first establish a relationship between the Legendre moments of the blurred image and those of the original image and the PSF. We then derive a set of blur moment invariants.

Legendre moments of the blurred image

The 2-D normalized Legendre moments of blurred image, $g(x, y)$, are defined by

$$\begin{aligned} L_{p,q}^{(g)} &= \int_{-1}^1 \int_{-1}^1 P_p(x) P_q(y) g(x, y) dx dy \\ &= \int_{-1}^1 \int_{-1}^1 P_p(x) P_q(y) (f * h)(x, y) dx dy \\ &= \int_{-1}^1 \int_{-1}^1 P_p(x) P_q(y) \left(\int_{-\infty}^{\infty} \int_{-\infty}^{\infty} h(a, b) f(x-a, y-b) da db \right) dx dy \\ &= \int_{-1}^1 \int_{-1}^1 h(a, b) \left(\int_{-1}^1 \int_{-1}^1 P_p(x+a) P_q(y+b) f(x, y) dx dy \right) da db. \end{aligned}$$

In the rest of this subsection, we discuss how to express the Legendre moments of blurred image defined by (12) in terms of Legendre moments of the original image and the PSF.

Making the notation $U_M(x) = (P_0(x), P_1(x), \dots, P_M(x))^T$ and $M_M(x) = (1, x, \dots, x^M)^T$ where the superscript T indicates the vector transposition, we have

$$U_M(x) = C_M M_M(x)$$

where $C_M = (c_{p,k})$, with $0 \leq k \leq p \leq M$, is a $(M+1) \times (M+1)$ lower triangular matrix whose elements $c_{p,k}$ are given by (10).

Since all the diagonal elements of C_M , $c_{pp} = \sqrt{\frac{2p+1}{2}}$, are not zero, the matrix C_M is non-singular, thus

$$M_M(x) = (C_M)^{-1} U_M(x) = D_M U_M(x)$$

where $D_M = (d_{p,k})$, with $0 \leq k \leq p \leq M$, is the inverse matrix of C_M . The elements of D_M are given by [29]

$$d_{p,k} = \begin{cases} \sqrt{\frac{2}{2k+1}} \frac{2^{\frac{3k-p}{2}} p! k!}{(\frac{p-k}{2})! \prod_{j=1}^{p-k} (2k+2j+1) (2k)!}, & p-k = \text{even} \\ 0, & p-k = \text{odd} \end{cases}$$

By expanding (14), we obtain

$$x^k = \sum_{i=0}^k d_{k,i} P_i(x)$$

Similarly,

$$a^m = \sum_{s=0}^m d_{m,s} P_s(a)$$

Replacing the variable x by x+a in (9), we have

$$P_p(x+a) = \sum_{m=0}^p c_{p,m} (x+a)^m = \sum_{m=0}^p \sum_{k=0}^m \binom{m}{k} c_{p,m} x^k a^{m-k}$$

Substitution of (16) and (17) into (18) yields

$$\begin{aligned} P_p(x+a) &= \sum_{m=0}^p \sum_{k=0}^m \binom{m}{k} c_{p,m} \sum_{i=0}^k d_{k,i} P_i(x) \sum_{s=0}^{m-k} d_{m-k,s} P_s(a) \\ &= \sum_{m=0}^p \sum_{k=0}^m \sum_{i=0}^k \sum_{s=0}^{m-k} \binom{m}{k} c_{p,m} d_{k,i} d_{m-k,s} P_i(x) P_s(a) \\ &= \sum_{i=0}^p \sum_{k=i}^p \sum_{m=k}^p \sum_{s=0}^{m-k} \binom{m}{k} c_{p,m} d_{k,i} d_{m-k,s} P_i(x) P_s(a) \end{aligned}$$

Similarly, we have

$$P_q(y+b) = \sum_{j=0}^q \sum_{n=j}^q \sum_{l=n}^q \sum_{t=0}^{n-l} \binom{n}{l} c_{q,n} d_{l,j} d_{n-l,t} P_j(y) P_t(b)$$

The following theorem reveals the relationship between the Legendre moments of the blurred image and those of the original image and the PSF.

Theorem 1

Let $f(x, y)$ be the original image function and the PSF $h(x, y)$ be an arbitrary image function, and $g(x, y)$ be a blurred version of $f(x, y)$, then the relations

$$L_{p,q}^{(g)} = \sum_{i=0}^p \sum_{j=0}^q L_{i,j}^{(f)} \sum_{s=0}^{p-i} \sum_{t=0}^{q-j} L_{s,t}^{(h)} \sum_{k=i}^{p-s} \sum_{m=k+s}^p \sum_{l=j}^{q-t} \sum_{n=l+t}^q \binom{m}{k} \binom{n}{l} c_{p,m} c_{q,n} d_{k,i} d_{m-k,s} d_{l,j} d_{n-l,t}$$

and

$$L_{p,q}^{(g)} = \sum_{i=0}^p \sum_{j=0}^q L_{i,j}^{(f)} \sum_{s=0}^{p-i} \sum_{t=0}^{q-j} L_{s,t}^{(h)} \sum_{k=i}^{p-s} \sum_{m=k+s}^p \sum_{l=j}^{q-t} \sum_{n=l+t}^q \binom{m}{k} \binom{n}{l} c_{p,m} c_{q,n} d_{k,i} d_{m-k,s} d_{l,j} d_{n-l,t}$$

hold for every p and q .

Proof

Substituting (19) and (20) into (12), we have

$$\int_{-1}^1 \int_{-1}^1 h(a, b) \left(\int_{-1}^1 \int_{-1}^1 \sum_{i=0}^p \sum_{k=i}^p \sum_{m=k}^p \sum_{s=0}^{m-k} \binom{m}{k} c_{p,m} d_{k,i} d_{m-k,s} P_i(x) P_s(a) \right) \times \left(\sum_{j=0}^q \sum_{n=j}^q \sum_{l=n}^q \sum_{t=0}^{n-l} \binom{n}{l} c_{q,n} d_{l,j} d_{n-l,t} P_j(y) P_t(b) \right) f(x, y) dx dy$$

The above equation can be rewritten as

$$\begin{aligned}
L_{p,q}^{(g)} &= \sum_{i=0}^p \sum_{k=i}^p \sum_{m=k}^p \sum_{s=0}^{m-k} \sum_{j=0}^q \sum_{l=j}^q \sum_{r=l}^q \sum_{t=0}^{r-l} \binom{m}{k} \binom{n}{l} C_{p,m} d_{m-k,s} d_{k,i} C_{q,n} d_{r-l,t} d_{i,j} L_{i,j}^f L_{s,t}^h \\
&= \sum_{i=0}^p \sum_{j=0}^q L_{i,j}^{(f)} \sum_{s=0}^{p-i} \sum_{t=0}^{q-j} L_{s,t}^{(h)} \sum_{k=i}^{p-s} \sum_{m=k+s}^p \sum_{l=j}^{q-t} \sum_{r=l+t}^q \binom{m}{k} \binom{n}{l} C_{p,m} C_{q,n} d_{k,i} d_{m-k,s} d_{l,j} d_{r-l,t}
\end{aligned}$$

The proof of (21) is now complete. The proof of (22) is very similar to that of (21), it is omitted here.

Theorem 2

If $h(x, y)$ satisfies the conditions of central symmetry, then

- $L_{p,q}^{(h)} = L_{p,q}^{(h)}$ for every p and q ;
- If $(p+q)$ is odd, then $L_{p,q}^{(h)} = 0$.

Proof

Using Lemma 1, the assertion of (a) can be easily proven. To demonstrate (b), it is noticed that $P_p(-x) = (-1)^p P_p(x)$. Using this relationship, we can deduce the result.

Blur invariants of Legendre moments

With the help of Theorems 1 and 2, we are now ready to construct a set of blur invariants of Legendre moments through the following theorem.

Theorem 3

Let $f(x, y)$ be an image function. Let us define the following function $I^{(f)}: \mathbf{N} \times \mathbf{N} \rightarrow \mathbf{R}$.

If $(p+q)$ is even then

$$I(p, q)^{(f)} = 0$$

If $(p+q)$ is odd then

$$I(p, q)^{(f)} = L_{p,q}^{(f)} - \frac{1}{2L_{0,0}^{(f)}} \sum_{i=0}^p \sum_{j=0}^q I(i, j)^{(f)} \sum_{s=0}^{p-i} \sum_{t=0}^{q-j} L_{s,t}^{(f)} \sum_{k=i}^{p-s} \sum_{m=k+s}^p \sum_{l=j}^{q-t} \sum_{r=l+t}^q \binom{m}{k} \binom{n}{l} C_{p,m} C_{q,n} d_{k,i} d_{m-k,s} d_{l,j} d_{r-l,t}$$

Then, $I(p, q)$ is invariant to centrally symmetric blur for any p and q . The number $p+q$ is called the order of the invariant.

The proof of Theorem 3 is given in Appendix A.

Using the Legendre central moments instead of Legendre moments, we can obtain a set of invariants to translation and to blur which are formally similar to $I(p, q)^{(f)}$.

Theorem 4

Let $f(x, y)$ be an image function. Let us define the following function $I^{(f)}: \mathbf{N} \times \mathbf{N} \rightarrow \mathbf{R}$.

If $(p+q)$ is even then

$$I(p, q)^{(f)} = 0.$$

If $(p+q)$ is odd then

$$I(p, q)^{(f)} = L_{p,q}^{(f)} - \frac{1}{2L_{0,0}^{(f)}} \sum_{i=0}^p \sum_{j=0}^q I(i, j)^{(f)} \sum_{s=0}^{p-i} \sum_{t=0}^{q-j} L_{s,t}^{(f)} \sum_{k=i}^{p-s} \sum_{m=k+s}^p \sum_{l=j}^{q-t} \sum_{r=l+t}^q \binom{m}{k} \binom{n}{l} C_{p,m} C_{q,n} d_{k,i} d_{m-k,s} d_{l,j} d_{r-l,t}$$

Then, $I(p, q)$ is invariant to centrally symmetric blur and to translation for any p and q .

The proof of Theorem 4 is very similar to that of Theorem 3, it is thus omitted here. It should be noted that $I(p, q)$ in (26) deals with translation of both the image and the PSF.

Based on (26), we can construct a set of blur and translation invariants of Legendre moments and express them in explicit form. The invariants of the third, fifth and seventh orders are listed in Appendix B.

EXPERIMENTAL RESULTS

In this section, some experiments are described in order to show the invariance of the proposed method to various PSF's and its robustness to different kinds of noise. The comparison with some existing methods in terms of recognition accuracy is also provided.

Test of invariance and robustness to noise

A toy cat image, whose size is 128×128 (Fig. 1), has been chosen from the public Columbia database [30]. This image was then successively degraded by out-of-focus blur, averaging mask, Gaussian function and motion filter as reported in [8], [9] and [19]. The parameter σ (standard deviation of the Gaussian function) of Gaussian blur was chosen equal to 0.5, and the parameter θ (θ means the angle in the counterclockwise direction, $\theta = 0$ corresponds to a horizontal motion, and $\theta = \pi/2$ corresponds to a vertical motion.) of motion blur set to 0. Other parameters such as the size for averaging blur, the radius for out-of-focus and the depth for motion filter were chosen equal to the size of blur mask in all the experiments. We first checked that the eighteen Legendre moment invariants of order up to seven (listed in Appendix B) were exactly equal to those of the original image whatever the blurring mode (the corresponding numerical values are omitted here).

Let us define the vectors $I_r = (I(0, r), I(1, r-1), \dots, I(r, 0))$ and $I(r) = (I_3, I_5, \dots, I_r)$ for any odd value of $r \geq 3$. The relative error between the two images is computed by

$$E_r(f, g) = \frac{\|\tilde{I}^{(f)}(r) - \tilde{I}^{(g)}(r)\|}{\|\tilde{I}^{(f)}(r)\|},$$

where $\|\cdot\|$ is Euclidean norm in L^2 space. In the following experiments, moment invariants of order up to $r = 7$ are used.

The next experiment was carried out to verify the performance of the invariants to both image blur and noise. The original cat image was blurred by a 9×9 averaging mask and a zero-mean Gaussian noise with standard deviation (STD) from 1 to 50 was added. Some examples of the blurred image with additive Gaussian noise or salt-and-pepper noise are shown in Fig. 2. Plots in Fig. 3 compare the relative error defined by (27) for Flusser's method based on geometric moment invariants (GMI) where eighteen blur invariants derived from central moments are used [7], the complex moment invariants (CMI) reported in [16] and the present Legendre moment invariants (LMI) up to order seven by averaging blur with different Gaussian noises. It can be seen from the figure that the proposed descriptors perform better than the GMI and CMI. Then, the cat image was blurred by a 11×11 motion filter, and the same Gaussian noise was added. The results (Fig. 4) again indicate the better behavior of the proposed method. Similarly, the original cat image was degraded on one hand by out-of-focus blur (13 pixel-radius of the PSF support) and by adding a salt-and-pepper noise with noise densities varying from 0.004 to 0.2 (see Fig. 5) and, on another hand, by Gaussian blur (the PSF was a Gaussian function with 15 pixel-radius of support) with the same salt-and-pepper noise (see Fig. 6). It can be also seen that a better robustness is achieved whatever the PSF or the additive noises.

Classification results

This experiment was carried out to compare the discrimination power of the GMI, CMI and LMI. A set of alphanumeric characters whose size is 50×50 pixels (Fig. 7) is used for the recognition task. The reason for choosing such a character set is that the elements in subset $\{0, o\}$, $\{2, Z\}$, $\{7, T\}$ and $\{9, q\}$ can be easily misclassified due to their similarity. The testing set is generated by adding averaging blur, out-of-focus blur, Gaussian blur and motion blur with mask of sizes 3×3 , 4×4 , 5×5 , 6×6 , 7×7 , 8×8 , 9×9 , 10×10 , 11×11 , 12×12 pixels, respectively. The parameter σ of Gaussian blur was chosen equal to 1 or 2, and the parameter θ of motion blur set to 0 or 1, forming a set of 480 images. Note that the original images as well as the blurred images are mapped onto the area of orthogonality, and the actual size of the blurred images in this experiment is 80×80 . This is followed by adding a white Gaussian noise with different standard deviations, salt-and-pepper noise with different noise densities and multiplicative noise with different noise densities. The Euclidean distance is used here as the classification measure. Table 1 shows the classification rates using the different moment invariants. One can observe from this table that the recognition results are quite good for the different methods in the noise-free case. The classification rates remain high for low and moderate noise levels but decrease significantly when the noise level goes up. However, if the GMI behaves better than the CMI, the LMI approach is the only one providing a rate close to or over 90% whatever the noise nature and its level.

In the next example, eight objects were selected from the Coil-100 image database of Columbia University as an original image set (see Fig. 8). The actual size of the blurred images in this experiment is 160×160. Fig. 9 shows some examples of the blurred and corrupted images. The recognition results are displayed in Table 2 . They lead to the same conclusions regarding the performance of the respective moment invariants but the decrease in recognition rate is more significant when the noise level is increased. This is also true for the LMI. The CMI do not perform well in these experiments due to their additional invariance to rotation. The worse numerical stability is a tax on the combined invariance. The orthogonality of LMI explains the difference in performance with GMI.

We also compared the computational load of the GMI, CMI and LMI in these two experiments. The programs were implemented in MATLAB 6.5 on a PC P4 2.4 GHZ, 512M RAM. It can be seen from Tables 1 and 2 that the GMI and the LMI computations are much faster than the CMI ones. This is due to the fact that the computation of the complex moments requires a mapping transformation which is time consuming.

Real image analysis

In the last experiment, we tested the performance of the invariants on images degraded by real out-of-focus blur. A sequence of eight pictures of a comb lying on a black ground was taken by a digital camera (Panasonic DMC-FZ50). The images differ from each other by the level of out-of-focus blur. The picture was captured 8 times from the same position but with different focus depth, manually set. All the test images are depicted in Fig. 10 . The values of GMI, CMI and LMI were computed for each image. Table 3 depicts the values of σ/μ , where μ denotes the mean of eight real images and σ the standard deviation. From this table, it can be seen that the minimal value of the LMI is 3.42% and the maximum value of the LMI is 6.15%, which are lower than those obtained with GMI (resp. 4.91%, 12.43%) and the CMI (resp. 7.47%, 7.54%).

Conclusion AND PERSPECTIVES

In this paper, we have proposed a new approach to derive a set of blur invariants using the orthogonal Legendre moments. The relationship between the Legendre moments of the blurred image and those of the original image and the PSF has been established, and using this relationship, a set of blur invariants based on Legendre moments has been derived. The experiments conducted so far in very distinct situations demonstrated that the proposed descriptors are more robust to noise and have better discriminative power than the methods based on geometric or complex moments.

One weak point of these descriptors is that they are only invariant to translation, but not invariant under image scaling and rotation. The derivation of combined invariants to both geometric transformation and blur is currently under investigation.

Acknowledgements:

This work was supported by the National Natural Science Foundation of China under Grant 60873048, by National Basic Research Program of China under grant No. 2010CB732503, Program for Changjiang Scholars and Innovative Research Team in University and the Natural Science Foundation of Jiangsu Province under Grant BK2008279.

The authors would like to thank the reviewers and Associate Editor Dr. Kuruoglu for their insightful suggestions which helped improve the manuscript.

Appendix A

The theoretical derivations provided here allow getting the expressions of the Legendre invariants to translation and blur. To prove Theorem 3, we need first the following Lemma.

Lemma 2

Let p, i, j and t be given integers satisfying $0 \leq i \leq p-1, 0 \leq j \leq p-i-1, 0 \leq t \leq p-i-j$, let us define

$$F(p, i, j, t) = \sum_{s=i+t}^{p-t} \sum_{l=j}^{s-j} \sum_{r=l+t}^s \sum_{k=s}^{p-t} \sum_{m=k+t}^p \binom{n}{l} \binom{m}{k} c_{s,n} d_{l,i} d_{r-l,j} c_{p,m} d_{k,s} d_{m-k,p}$$

$$G(p, i, j, t) = \sum_{s=j+t}^{p-i} \sum_{l=j}^{s-t} \sum_{r=l+t}^s \sum_{k=i}^{p-s} \sum_{m=k+s}^p \binom{n}{l} \binom{m}{k} c_{s,n} d_{l,j} d_{r-l,t} c_{p,m} d_{k,i} d_{m-k,s}$$

where the coefficients $c_{i,j}$ and $d_{m,n}$ are respectively given by (10) and (15), then we have $F(p, i, j, t) = G(p, i, j, t)$.

Proof

By changing the order of summation in (A1), we have

$$\begin{aligned} F(p, i, j, t) &= \sum_{m=0}^p c_{p,m} \sum_{l=0}^{p-t-j} \sum_{n=0}^{p-t} \sum_{k=0}^{p-t} \sum_{s=0}^{p-t} \binom{m}{k} \binom{n}{l} c_{s,n} d_{l,i} d_{n-l,j} d_{k,s} d_{m-k,t} \\ &= \sum_{m=0}^p c_{p,m} F_1(p, m, i, j, t) \end{aligned}$$

where

$$F_1(p, m, i, j, t) = \sum_{l=0}^{p-t-j} \sum_{n=0}^{p-t} \sum_{k=0}^{p-t} \sum_{s=0}^{p-t} \binom{m}{k} \binom{n}{l} c_{s,n} d_{l,i} d_{n-l,j} d_{k,s} d_{m-k,t}$$

Similarly, (A2) can be written as

$$\begin{aligned} G(p, i, j, t) &= \sum_{m=0}^p c_{p,m} \sum_{l=0}^{p-t-i} \sum_{n=0}^{p-i} \sum_{k=0}^p \sum_{s=0}^{p-i} \binom{m}{k} \binom{n}{l} c_{s,n} d_{l,j} d_{n-l,t} d_{k,i} d_{m-k,s} \\ &= \sum_{m=0}^p c_{p,m} G_1(p, m, i, j, t) \end{aligned}$$

where

$$G_1(p, m, i, j, t) = \sum_{l=0}^{p-t-i} \sum_{n=0}^{p-i} \sum_{k=0}^p \sum_{s=0}^{p-i} \binom{m}{k} \binom{n}{l} c_{s,n} d_{l,j} d_{n-l,t} d_{k,i} d_{m-k,s}$$

To prove the Lemma, it suffices to prove $F_1(p, m, i, j, t) = G_1(p, m, i, j, t)$. Since both $C_M = (c_{i,j})$ and $D_M = (d_{i,j})$ are lower triangular matrices, it is clear that $d_{k,s} = 0$ if $s > k$, and $c_{s,n} = 0$ if $n > s$. Using these properties and changing the order of summation in (A4) and (A6), we have

$$\begin{aligned} F_1(p, m, i, j, t) &= \sum_{k=0}^m \sum_{s=0}^k \sum_{n=0}^s \sum_{l=0}^n \binom{m}{k} \binom{n}{l} c_{s,n} d_{l,i} d_{n-l,j} d_{k,s} d_{m-k,t} \\ G_1(p, m, i, j, t) &= \sum_{k=0}^m \sum_{s=0}^{m-k} \sum_{n=0}^s \sum_{l=0}^n \binom{m}{k} \binom{n}{l} c_{s,n} d_{l,j} d_{n-l,t} d_{k,i} d_{m-k,s} \end{aligned}$$

(A7) can be further written as

$$\begin{aligned} F_1(p, m, i, j, t) &= \sum_{k=0}^{+\infty} \sum_{s=0}^{+\infty} \sum_{n=0}^{+\infty} \sum_{l=0}^{+\infty} \binom{m}{k} \binom{n}{l} c_{s,n} d_{l,i} d_{n-l,j} d_{k,s} d_{m-k,t} \\ &= \sum_{k=0}^{+\infty} \sum_{n=0}^{+\infty} \sum_{l=0}^{+\infty} \binom{m}{k} \binom{n}{l} d_{l,i} d_{n-l,j} d_{m-k,t} \sum_{s=0}^{+\infty} d_{k,s} c_{s,n} \end{aligned}$$

where the convention $\binom{m}{k} = 0$ if $k > m$ is used in the above equation.

Since the matrix D_M is the inverse of C_M , we have $\sum_{s=0}^{+\infty} d_{s,n} c_{s,n} = \delta_{n,0}$, thus, (A9) becomes

$$\begin{aligned} F_1(p, m, i, j, t) &= \sum_{k=0}^{+\infty} \sum_{l=0}^{+\infty} \binom{m}{k} \binom{l}{l} d_{l,i} d_{k-l,j} d_{m-k,t} \\ &= \sum_{k=0}^{+\infty} \sum_{l=0}^{+\infty} \frac{m!}{k!(m-k)!(k-l)!} d_{l,i} d_{k-l,j} d_{m-k,t} \end{aligned}$$

Letting $e_{u,v} = d_{u,v}/u!$, we have

$$F_1(p, m, i, j, t) = m! \sum_{k=0}^{+\infty} \sum_{l=0}^{+\infty} e_{l,i} e_{k-l,j} e_{m-k,t} = m! \sum_{k=0}^{+\infty} \sum_{l=0}^{+\infty} e_{m-k-l,i} e_{l,j} e_{k,t}$$

From the above equation, it can easily be obtained

$$F_{\mathbb{1}}(p, m, i, t, j) = m! \sum_{k=0}^{+\infty} \sum_{l=0}^{+\infty} e_{m-k-l, i} e_{l, t} e_{k, j} = m! \sum_{k=0}^{+\infty} \sum_{l=0}^{+\infty} e_{m-k-l, i} e_{k, t} e_{l, j}$$

$$= F_{\mathbb{1}}(p, m, i, j, t) \quad (\text{making the change of variables } k = l \text{ and } l = k)$$

Making the change of variable $l = n - 1$ in (A7), we can deduce

$$F_{\mathbb{1}}(p, m, i, j, t) = F_{\mathbb{1}}(p, m, j, i, t)$$

Combining (A12) and (A13) and using (A7), we obtain

$$F_{\mathbb{1}}(p, m, i, j, t) = F_{\mathbb{1}}(p, m, j, t, i) = \sum_{k=0}^m \sum_{s=0}^k \sum_{r=0}^s \sum_{l=0}^n \binom{m \setminus n}{k \setminus l} c_{s, n} d_{l, j} d_{n-l, t} d_{k, s} d_{m-k, i}$$

$$= \sum_{k=0}^m \sum_{s=0}^k \sum_{r=0}^s \sum_{l=0}^n \binom{m}{m-k} \binom{n}{l} c_{s, n} d_{l, j} d_{n-l, t} d_{m-k, s} d_{k, i} \quad (\text{making the change of variable } k = m - k)$$

$$= \sum_{k=0}^m \sum_{s=0}^k \sum_{r=0}^s \sum_{l=0}^n \binom{m \setminus n}{k \setminus l} c_{s, n} d_{l, j} d_{n-l, t} d_{k, i} d_{m-k, s}$$

$$= G_{\mathbb{1}}(p, m, i, j, t)$$

The proof of Lemma 2 is now complete.

Proof of Theorem 3

We only need to prove the Theorem for the case where $p+q$ is odd. We will do this by mathematical induction. It can be easily verified that the result is true for $p+q = 1$. For $p+q = 3$, four cases need to be considered: (1) ($p = 3, q = 0$); (2) ($p = 2, q = 1$); (3) ($p = 1, q = 2$); (4) ($p = 0, q = 3$). We provide here the demonstration for $p = 2$ and $q = 1$, other cases can be proved in a similar manner. We deduce from (25) that

$$\sum_{i=0}^2 \sum_{j=0}^1 \sum_{0 < i+j < 3} I(i, j)^{(g)} \sum_{s=0}^{2-i} \sum_{t=0}^{1-j} L_{s, t}^{(f)} \sum_{k=i}^{2-s} \sum_{m=k+s}^2 \sum_{l=j}^{1-t} \sum_{n=l+t}^1 \binom{m \setminus n}{k \setminus l} c_{2m} c_{1n} d_{k, i} d_{m-k, s} d_{l, j} d_{n-l, t}$$

$$)^{(g)} \sum_{s=0}^1 \sum_{t=0}^1 L_{s, t}^{(f)} \sum_{k=1}^{2-s} \sum_{m=k+s}^2 \sum_{l=0}^{1-t} \sum_{n=l+t}^1 \binom{m \setminus n}{k \setminus l} c_{2m} c_{1n} d_{k, 1} d_{m-k, s} d_{l, 0} d_{n-l, t} + I(0, 1)^{(g)} \sum_{s=0}^2 L_{s, 0}^{(f)} \sum_{k=0}^{2-s} \sum_{m=k+s}^2 \binom{m}{k} c_{2m} c_{1n}$$

Using Theorem 2, it can be obtained from (21) that

$$L_{0,0}^{(g)} = L_{0,0}^{(f)}$$

$$L_{1,0}^{(g)} = L_{1,0}^{(f)} \quad L_{0,1}^{(g)} = L_{0,1}^{(f)}$$

$$L_{2,0}^{(g)} = L_{2,0}^{(f)} + 2L_{0,0}^{(f)} L_{2,0}^{(f)} + \sqrt{5} L_{0,0}^{(f)} L_{0,0}^{(f)}$$

$$L_{1,1}^{(g)} = L_{1,1}^{(f)} + 2L_{0,0}^{(f)} L_{1,1}^{(f)}$$

$$L_{2,1}^{(g)} = L_{2,1}^{(f)} + 2\sqrt{5} L_{1,0}^{(f)} L_{1,1}^{(f)} + 2L_{0,1}^{(f)} L_{2,0}^{(f)} - \sqrt{5} L_{0,1}^{(f)} L_{0,0}^{(f)}$$

Substituting the above equations into (A15) and using the relationships $I(1, 0)^{(g)} = I(1, 0)^{(f)} = L_{1,0}^{(f)}$ and $I(0, 1)^{(g)} = I(0, 1)^{(f)} = L_{0,1}^{(f)}$, we have $I(2, 1)^{(g)} = I(2, 1)^{(f)}$.

Suppose that Theorem 3 is valid for all invariants of order up to $p+q-2$, then we get

$$\begin{aligned}
& I(p, q)^{(g)} - I(p, q)^{(f)} \\
&= L_{p,q}^{(g)} - \frac{1}{2L_{0,0}^{(g)}} \sum_{i=0}^p \sum_{j=0}^q I(i, j)^{(g)} \sum_{s=0}^{p-i} \sum_{t=0}^{q-j} L_{s,t}^{(g)} \sum_{k=i}^{p-s} \sum_{m=k+s}^p \sum_{l=j}^{q-t} \sum_{n=l+t}^q \binom{m}{k} \binom{n}{l} c_{p,m} c_{q,n} d_{k,i} d_{m-k,s} d_{l,j} d_{n-l,t} \\
&- L_{p,q}^{(f)} + \frac{1}{2L_{0,0}^{(f)}} \sum_{i=0}^p \sum_{j=0}^q I(i, j)^{(f)} \sum_{s=0}^{p-i} \sum_{t=0}^{q-j} L_{s,t}^{(f)} \sum_{k=i}^{p-s} \sum_{m=k+s}^p \sum_{l=j}^{q-t} \sum_{n=l+t}^q \binom{m}{k} \binom{n}{l} c_{p,m} c_{q,n} d_{k,i} d_{m-k,s} d_{l,j} d_{n-l,t} \\
&= L_{p,q}^{(g)} - L_{p,q}^{(f)} \\
&- \frac{1}{2L_{0,0}^{(f)}} \sum_{i=0}^p \sum_{j=0}^q I(i, j)^{(f)} \sum_{s=0}^{p-i} \sum_{t=0}^{q-j} (L_{s,t}^{(g)} - L_{s,t}^{(f)}) \sum_{k=i}^{p-s} \sum_{m=k+s}^p \sum_{l=j}^{q-t} \sum_{n=l+t}^q \binom{m}{k} \binom{n}{l} c_{p,m} c_{q,n} d_{k,i} d_{m-k,s} d_{l,j} d_{n-l,t}
\end{aligned}$$

Using the property $(d_{0,0})^2 = 2$, equation (25) can be rewritten as

$$L_{p,q}^{(f)} = \frac{1}{2L_{0,0}^{(f)}} \sum_{i=0}^p \sum_{j=0}^q I(i, j)^{(f)} \sum_{s=0}^{p-i} \sum_{t=0}^{q-j} L_{s,t}^{(f)} \sum_{k=i}^{p-s} \sum_{m=k+s}^p \sum_{l=j}^{q-t} \sum_{n=l+t}^q \binom{m}{k} \binom{n}{l} c_{p,m} c_{q,n} d_{k,i} d_{m-k,s} d_{l,j} d_{n-l,t}$$

Using (21), we have

$$\begin{aligned}
L_{p,q}^{(g)} - L_{p,q}^{(f)} &= \sum_{i=0}^p \sum_{j=0}^q L_{i,j}^{(f)} \sum_{s=0}^{p-i} \sum_{t=0}^{q-j} L_{s,t}^{(g)} \sum_{k=i}^{p-s} \sum_{m=k+s}^p \sum_{l=j}^{q-t} \sum_{n=l+t}^q \binom{m}{k} \binom{n}{l} c_{p,m} c_{q,n} d_{k,i} d_{m-k,s} d_{l,j} d_{n-l,t} - L_{p,q}^{(f)} \\
&= \sum_{i=0}^p \sum_{j=0}^q L_{i,j}^{(f)} \sum_{s=0}^{p-i} \sum_{t=0}^{q-j} L_{s,t}^{(g)} \sum_{k=i}^{p-s} \sum_{m=k+s}^p \sum_{l=j}^{q-t} \sum_{n=l+t}^q \binom{m}{k} \binom{n}{l} c_{p,m} c_{q,n} d_{k,i} d_{m-k,s} d_{l,j} d_{n-l,t} \\
&= \sum_{i=0}^p \sum_{j=0}^q L_{i,j}^{(f)} \sum_{s=0}^{p-i} \sum_{t=0}^{q-j} L_{s,t}^{(g)} A(p, q, i, j, s, t)
\end{aligned}$$

where

$$A(p, q, i, j, s, t) = \sum_{k=i}^{p-s} \sum_{m=k+s}^p \sum_{l=j}^{q-t} \sum_{n=l+t}^q \binom{m}{k} \binom{n}{l} c_{p,m} c_{q,n} d_{k,i} d_{m-k,s} d_{l,j} d_{n-l,t}$$

Similarly

$$L_{s,t}^{(g)} - L_{s,t}^{(f)} = \sum_{i=0}^s \sum_{j=0}^t L_{i,j}^{(f)} \sum_{s=0}^{s-i} \sum_{t=0}^{t-j} L_{s',t'}^{(g)} A(s, t, i, j, s', t')$$

Substituting (A18) and (A20) into (A16) and using (A17), we obtain

$$\begin{aligned}
& I(p, q)^{(g)} - I(p, q)^{(f)} \\
&= \sum_{i=0}^p \sum_{\substack{j=0 \\ i+j < p+q}}^q L_{i,j}^{(f)} \sum_{s=0}^{p-i} \sum_{t=0}^{q-j} L_{s,t}^{(g)} A(p, q, i, j, s, t) \\
&- \frac{1}{2L_{0,0}^{(f)}} \sum_{i=0}^p \sum_{\substack{j=0 \\ i+j < p+q}}^q I(i, j)^{(f)} \sum_{s=0}^{p-i} \sum_{t=0}^{q-j} \left[\sum_{i=0}^s \sum_{j=0}^t L_{i,j}^{(f)} \sum_{s=0}^{s-i} \sum_{t=0}^{t-j} L_{s,t}^{(g)} A(s, t, i, j, s, t) \right] A(p, q, i, j, s, t) \\
&= \sum_{i=0}^p \sum_{\substack{j=0 \\ i+j < p+q}}^q \left[\frac{1}{2L_{0,0}^{(f)}} \sum_{i=0}^i \sum_{j=0}^j I(i, j)^{(f)} \sum_{s=0}^{i-i} \sum_{t=0}^{j-j} L_{s,t}^{(f)} A(i, j, i, j, s, t) \right] \sum_{s=0}^{p-i} \sum_{t=0}^{q-j} L_{s,t}^{(g)} A(p, q, i, j, s, t) \\
&- \frac{1}{2L_{0,0}^{(f)}} \sum_{i=0}^p \sum_{\substack{j=0 \\ i+j < p+q}}^q I(i, j)^{(f)} \sum_{s=0}^{p-i} \sum_{t=0}^{q-j} \left[\sum_{i=0}^s \sum_{j=0}^t L_{i,j}^{(f)} \sum_{s=0}^{s-i} \sum_{t=0}^{t-j} L_{s,t}^{(g)} A(s, t, i, j, s, t) \right] A(p, q, i, j, s, t) \\
&= \frac{1}{2L_{0,0}^{(f)}} \sum_{i=0}^p \sum_{\substack{j=0 \\ i+j < p+q}}^q I(i, j)^{(f)} \sum_{i=i}^p \sum_{\substack{j=j \\ i+j < p+q}}^q \sum_{s=0}^{i-i} \sum_{t=0}^{j-j} L_{s,t}^{(f)} A(i, j, i, j, s, t) \sum_{s=0}^{p-i} \sum_{t=0}^{q-j} L_{s,t}^{(g)} A(p, q, i, j, s, t) \\
&- \frac{1}{2L_{0,0}^{(f)}} \sum_{i=0}^p \sum_{\substack{j=0 \\ i+j < p+q}}^q I(i, j)^{(f)} \sum_{s=0}^{p-i} \sum_{t=0}^{q-j} \left[\sum_{i=0}^s \sum_{j=0}^t L_{i,j}^{(f)} \sum_{s=0}^{s-i} \sum_{t=0}^{t-j} L_{s,t}^{(g)} A(s, t, i, j, s, t) \right] A(p, q, i, j, s, t)
\end{aligned}$$

Define

$$\begin{aligned}
B(p, q) &= \frac{1}{2L_{0,0}^{(f)}} \sum_{i=0}^p \sum_{\substack{j=0 \\ i+j < p+q}}^q I(i, j)^{(f)} \sum_{s=0}^{p-i} \sum_{t=0}^{q-j} L_{s,t}^{(f)} L_{0,0}^{(g)} A(p, q, i, j, s, t) A(p, q, p, q, 0, 0) \\
&= \frac{1}{2L_{0,0}^{(f)}} \sum_{i=0}^p \sum_{\substack{j=0 \\ i+j < p+q}}^q I(i, j)^{(f)} \sum_{s=0}^{p-i} \sum_{t=0}^{q-j} L_{s,t}^{(f)} L_{0,0}^{(g)} A(p, q, i, j, s, t) A(p, q, p, q, 0, 0) \\
B(p, q) &= \frac{1}{2L_{0,0}^{(f)}} \sum_{i=0}^p \sum_{\substack{j=0 \\ i+j < p+q}}^q I(i, j)^{(f)} \sum_{s=0}^{p-i} \sum_{t=0}^{q-j} L_{s,t}^{(f)} L_{0,0}^{(g)} A(p, q, i, j, s, t) A(s, t, s, t, 0, 0),
\end{aligned}$$

it can be easily verified from (A19) that $A(p, q, p, q, 0, 0) = A(s, t, s, t, 0, 0) = (d_{0,0})^2$, thus, we have $B(p, q) = B'(p, q)$. Using this relationship, (A21) can be rewritten as

$$\begin{aligned}
& I(p, q)^{(g)} - I(p, q)^{(f)} \\
&= \frac{1}{2L_{0,0}^{(f)}} \sum_{i=0}^p \sum_{\substack{j=0 \\ i+j < p+q}}^q I(i, j)^{(f)} \sum_{i=i}^p \sum_{\substack{j=j \\ i+j < p+q}}^q \sum_{s=0}^{i-i} \sum_{t=0}^{j-j} L_{s,t}^{(f)} A(i, j, i, j, s, t) \sum_{s=0}^{p-i} \sum_{t=0}^{q-j} L_{s,t}^{(g)} A(p, q, i, j, s, t) \\
&- \frac{1}{2L_{0,0}^{(f)}} \sum_{i=0}^p \sum_{\substack{j=0 \\ i+j < p+q}}^q I(i, j)^{(f)} \sum_{s=0}^{p-i} \sum_{t=0}^{q-j} \left[\sum_{i=0}^s \sum_{j=0}^t L_{i,j}^{(f)} \sum_{s=0}^{s-i} \sum_{t=0}^{t-j} L_{s,t}^{(g)} A(s, t, i, j, s, t) \right] A(p, q, i, j, s, t)
\end{aligned}$$

Changing the order of summation and shifting the indices in the above equation, we obtain

$$\begin{aligned}
& I(p, q)^{(g)} - I(p, q)^{(f)} \\
&= \frac{1}{2L_{q,0}^{(f)}} \sum_{i=0}^p \sum_{\substack{j=0 \\ i+j < p+q}}^q I(i, j)^{(f)} \sum_{s=0}^{p-i} \sum_{t=0}^{q-j} L_{s,t}^{(f)} \sum_{s=0}^{p-i-s} \sum_{t=0}^{q-j-t} L_{s,t}^{(g)} \sum_{i=i+s}^{p-s} \sum_{j=j+t}^{q-t} A(i, j, i, j, s', t) A(p, q, i, j, s, t) \\
&- \frac{1}{2L_{q,0}^{(f)}} \sum_{i=0}^p \sum_{\substack{j=0 \\ i+j < p+q}}^q I(i, j)^{(f)} \sum_{i=0}^{p-i} \sum_{j=0}^{q-j} L_{i,j}^{(f)} \sum_{s=0}^{p-i-i} \sum_{t=0}^{q-j-j} L_{s,t}^{(g)} \sum_{s=i+s}^{p-i} \sum_{t=j+t}^{q-i} A(s, t, i, j, s', t) A(p, q, i, j, s, t) \\
&= \frac{1}{2L_{q,0}^{(f)}} \sum_{i=0}^p \sum_{\substack{j=0 \\ i+j < p+q}}^q I(i, j)^{(f)} \sum_{i=0}^{p-i} \sum_{j=0}^{q-j} L_{i,j}^{(f)} \sum_{s=0}^{p-i-i} \sum_{t=0}^{q-j-j} L_{s,t}^{(g)} \sum_{s=i+t}^{p-s} \sum_{t=j+j}^{q-t} A(s, t, i, j, i, j) A(p, q, s, t, s, t) \\
&- \frac{1}{2L_{q,0}^{(f)}} \sum_{i=0}^p \sum_{\substack{j=0 \\ i+j < p+q}}^q I(i, j)^{(f)} \sum_{i=0}^{p-i} \sum_{j=0}^{q-j} L_{i,j}^{(f)} \sum_{s=0}^{p-i-i} \sum_{t=0}^{q-j-j} L_{s,t}^{(g)} \sum_{s=i+s}^{p-i} \sum_{t=j+t}^{q-j} A(s, t, i, j, s, t) A(p, q, i, j, s, t) \\
&= \frac{1}{2L_{q,0}^{(f)}} \sum_{i=0}^p \sum_{\substack{j=0 \\ i+j < p+q}}^q I(i, j)^{(f)} \sum_{i=0}^{p-i} \sum_{j=0}^{q-j} L_{i,j}^{(f)} \sum_{s=0}^{p-i-i} \sum_{t=0}^{q-j-j} L_{s,t}^{(g)} T(p, q, i, j, i, j, s, t)
\end{aligned}$$

where

$$T(p, q, i, j, i, j, s, t) = \sum_{s=i+t}^{p-s} \sum_{t=j+j}^{q-t} A(s, t, i, j, i, j) A(p, q, s, t, s, t) - \sum_{s=i+s}^{p-i} \sum_{t=j+t}^{q-j} A(s, t, i, j, s, t) A(p, q, i, j, s, t)$$

Using (A19), we have

$$\begin{aligned}
& T(p, q, i, j, i, j, s, t) \\
&= \sum_{s=i+t}^{p-s} \sum_{t=j+j}^{q-t} \sum_{k=i}^{s-i} \sum_{m=k+i}^s \sum_{l=j}^{t-j} \sum_{n=l+t}^{t'} \binom{m}{k} \binom{n}{l} c_{s,m} c_{t,n} d_{k,i} d_{m-k,i} d_{l,j} d_{n-l,j} \\
&\times \sum_{k=s}^{p-s} \sum_{m=k+s}^p \sum_{l=t}^{q-t} \sum_{n=l+t}^q \binom{m}{k} \binom{n}{l} c_{p,m} c_{q,n} d_{k,s} d_{m-k,s} d_{l,t} d_{n-l,t} \\
&- \sum_{s=i+s}^{p-i} \sum_{t=j+t}^{q-j} \sum_{k=i}^{s-s} \sum_{m=k+s}^s \sum_{l=j}^{t-t} \sum_{n=l+t}^{t'} \binom{m}{k} \binom{n}{l} c_{s,m} c_{t,n} d_{k,i} d_{m-k,i} d_{l,j} d_{n-l,t} \\
&\times \sum_{k=i}^{p-s} \sum_{m=k+s}^p \sum_{l=j}^{q-t} \sum_{n=l+t}^q \binom{m}{k} \binom{n}{l} c_{p,m} c_{q,n} d_{k,i} d_{m-k,s} d_{l,j} d_{n-l,t} \\
&= \sum_{s=i+t}^{p-s} \sum_{k=i}^{s-i} \sum_{m=k+i}^s \sum_{k=s}^{p-s} \sum_{m=k+s}^p \binom{m}{k} \binom{m}{k} c_{s,m} c_{k,i} d_{m-k,i} c_{p,m} d_{k,s} d_{m-k,s} \\
&\times \sum_{t=j+j}^{q-t} \sum_{l=j}^{t-j} \sum_{n=l+j}^{t'} \sum_{l=t}^{q-t} \sum_{n=l+t}^q \binom{n}{l} \binom{n}{l} c_{t,n} d_{l,j} d_{n-l,t} c_{q,n} d_{l,t} d_{n-l,t} \\
&- \sum_{s=i+s}^{p-i} \sum_{k=i}^{s-s} \sum_{m=k+s}^s \sum_{k=i}^{p-s} \sum_{m=k+s}^p \binom{m}{k} \binom{m}{k} c_{s,m} d_{k,i} d_{m-k,s} c_{p,m} d_{k,i} d_{m-k,s} \\
&\times \sum_{t=j+t}^{q-j} \sum_{l=j}^{t-t} \sum_{n=l+t}^{t'} \sum_{l=j}^{q-t} \sum_{n=l+t}^q \binom{n}{l} \binom{n}{l} c_{t,n} d_{l,j} d_{n-l,t} c_{q,n} d_{l,t} d_{n-l,t} \\
&= F(p, i, i, s) F(q, j, j, t) - G(p, i, i, s) G(q, j, j, t)
\end{aligned}$$

where $F(p, i, i, s)$ and $G(p, i, i, s)$ are respectively given by (A1) and (A2).

Using Lemma 2, we have

$$T(p, q, i, j, i, j, s, t) = 0.$$

Thus

$$I(p, q)^{(g)} - I(p, q)^{(f)} = 0$$

The proof of Theorem 3 has been completed.

Appendix B: LIST OF LEGENDRE MOMENT INVARIANTS UP TO THE SEVENTH ORDER

The expressions given below provide to the interested readers all the elements to replicate our method and to apply it to other examples.

- Third order

$$\bar{I}(3, 0) = \bar{L}_{30}$$

$$\bar{I}(2, 1) = \bar{L}_{21}$$

$$\bar{I}(1, 2) = L_{12}$$

$$\bar{I}(0, 3) = L_{03}$$

- Fifth order

$$\begin{aligned} \bar{I}(5, 0) &= L_{50} - \frac{3\sqrt{77}}{2} L_{30} - \frac{3\sqrt{385} L_{20} L_{30}}{5L_{00}} \\ \bar{I}(4, 1) &= \bar{L}_{41} - \frac{7\sqrt{5}}{2} \bar{L}_{21} - \frac{1}{L_{00}} (7\bar{L}_{21}\bar{L}_{20} + \sqrt{21}\bar{L}_{11}\bar{L}_{30}) \\ \bar{I}(3, 2) &= L_{32} - \frac{5}{6}\sqrt{21}L_{12} - \frac{\sqrt{5}}{2} L_{30} - \frac{1}{L_{00}} \left(\frac{\sqrt{105}}{3} L_{20}L_{12} + \frac{5\sqrt{21}}{3} L_{11}L_{21} + L_{02}L_{30} \right) \\ \bar{I}(2, 3) &= \bar{L}_{23} - \frac{5}{6}\sqrt{21}\bar{L}_{21} - \frac{\sqrt{5}}{2} \bar{L}_{03} - \frac{1}{L_{00}} \left(\frac{\sqrt{105}}{3} \bar{L}_{02}\bar{L}_{21} + \frac{5\sqrt{21}}{3} \bar{L}_{11}\bar{L}_{12} + \bar{L}_{20}\bar{L}_{03} \right) \\ \bar{I}(1, 4) &= L_{14} - \frac{7\sqrt{5}}{2} L_{12} - \frac{1}{L_{00}} (7L_{12}L_{02} + \sqrt{21}L_{11}L_{03}) \\ \bar{I}(0, 5) &= \bar{L}_{05} - \frac{3\sqrt{77}}{2} \bar{L}_{03} - \frac{3\sqrt{385} L_{02} L_{03}}{5L_{00}} \end{aligned}$$

- Seventh order

$$\begin{aligned}
\bar{I}(7, 0) &= \bar{L}_{70} - \frac{1727\sqrt{105}}{120} \bar{L}_{30} - \frac{13\sqrt{165}}{6} \bar{I}(5, 0) \\
&\quad - \frac{1}{L_{00}} \left(\frac{1595\sqrt{21}}{42} \bar{L}_{20} \bar{L}_{30} + \frac{143\sqrt{105}}{35} \bar{L}_{40} \bar{L}_{30} + \frac{13\sqrt{33}}{3} \bar{L}_{20} \bar{I}(5, 0) \right) \\
\bar{I}(6, 1) &= L_{61} - \frac{351\sqrt{65}}{40} L_{21} - \frac{11\sqrt{13}}{2} \bar{I}(4, 1) - \frac{1}{L_{00}} \left(\frac{45\sqrt{13}}{2} L_{20} L_{21} + \frac{11\sqrt{65}}{5} L_{40} L_{21} \right. \\
&\quad \left. + \frac{109\sqrt{273}}{30} L_{11} L_{30} + \frac{33\sqrt{13}}{5} L_{31} L_{30} + \frac{11\sqrt{65}}{5} L_{20} \bar{I}(4, 1) + \frac{\sqrt{429}}{3} L_{11} \bar{I}(5, 0) \right) \\
\bar{I}(5, 2) &= \bar{L}_{52} - \frac{119\sqrt{33}}{24} \bar{L}_{12} - \frac{3\sqrt{385}}{4} \bar{L}_{30} - \frac{3\sqrt{77}}{2} \bar{I}(3, 2) - \frac{\sqrt{5}}{2} \bar{I}(5, 0) \\
&\quad - \frac{1}{L_{00}} \left(\frac{73\sqrt{165}}{30} L_{20} L_{12} + \sqrt{33} L_{40} L_{12} + \frac{73\sqrt{33}}{6} L_{11} L_{21} + 3\sqrt{77} L_{31} L_{21} + \frac{3\sqrt{77}}{2} L_{02} L_{30} \right. \\
&\quad \left. + \frac{3\sqrt{77}}{2} \bar{L}_{20} \bar{L}_{30} + \frac{3\sqrt{385}}{5} \bar{L}_{22} \bar{L}_{30} + \frac{3\sqrt{385}}{5} \bar{L}_{20} \bar{I}(3, 2) + \sqrt{165} \bar{L}_{11} \bar{I}(4, 1) + \bar{L}_{02} \bar{I}(5, 0) \right) \\
\bar{I}(4, 3) &= L_{43} - \frac{61}{8} L_{03} - \frac{35\sqrt{105}}{12} L_{21} - \frac{7\sqrt{5}}{2} \bar{I}(2, 3) - \frac{5\sqrt{21}}{6} \bar{I}(4, 1) \\
&\quad - \frac{1}{L_{00}} \left(\frac{7\sqrt{5}}{2} L_{20} L_{03} + L_{40} L_{03} + \frac{9\sqrt{105}}{2} L_{11} L_{12} + 7\sqrt{5} L_{31} L_{12} + \frac{35\sqrt{21}}{6} L_{02} L_{21} + \frac{35\sqrt{21}}{6} L_{20} L_{21} \right. \\
&\quad \left. + \frac{7\sqrt{105}}{3} L_{22} L_{21} + 7L_{20} \bar{I}(2, 3) + \frac{35}{2} L_{11} L_{30} + \sqrt{21} L_{13} L_{30} + 7\sqrt{5} L_{11} \bar{I}(3, 2) + \frac{\sqrt{105}}{3} L_{02} \bar{I}(4, 1) \right) \\
\bar{I}(3, 4) &= \bar{L}_{34} - \frac{61}{8} \bar{L}_{30} - \frac{35\sqrt{105}}{12} \bar{L}_{12} - \frac{7\sqrt{5}}{2} \bar{I}(3, 2) - \frac{5\sqrt{21}}{6} \bar{I}(1, 4) \\
&\quad - \frac{1}{L_{00}} \left(\frac{7\sqrt{5}}{2} \bar{L}_{02} \bar{L}_{30} + \bar{L}_{04} \bar{L}_{30} + \frac{9\sqrt{105}}{2} \bar{L}_{11} \bar{L}_{21} + 7\sqrt{5} \bar{L}_{13} \bar{L}_{21} + \frac{35\sqrt{21}}{6} \bar{L}_{20} \bar{L}_{12} + \frac{35\sqrt{21}}{6} \bar{L}_{02} \bar{L}_{12} \right. \\
&\quad \left. + \frac{7\sqrt{105}}{3} \bar{L}_{22} \bar{L}_{12} + 7\bar{L}_{02} \bar{I}(3, 2) + \frac{35}{2} \bar{L}_{11} \bar{L}_{03} + \sqrt{21} \bar{L}_{31} \bar{L}_{03} + 7\sqrt{5} \bar{L}_{11} \bar{I}(2, 3) + \frac{\sqrt{105}}{3} \bar{L}_{20} \bar{I}(1, 4) \right) \\
\bar{I}(2, 5) &= L_{25} - \frac{119\sqrt{33}}{24} L_{21} - \frac{3\sqrt{385}}{4} L_{03} - \frac{3\sqrt{77}}{2} \bar{I}(2, 3) - \frac{\sqrt{5}}{2} \bar{I}(0, 5) \\
&\quad - \frac{1}{L_{00}} \left(\frac{73\sqrt{165}}{30} L_{02} L_{21} + \sqrt{33} L_{04} L_{21} + \frac{73\sqrt{33}}{6} L_{11} L_{12} + 3\sqrt{77} L_{13} L_{12} + \frac{3\sqrt{77}}{2} L_{20} L_{03} \right. \\
&\quad \left. + \frac{3\sqrt{77}}{2} L_{02} L_{03} + \frac{3\sqrt{385}}{5} L_{22} L_{03} + \frac{3\sqrt{385}}{5} L_{02} \bar{I}(2, 3) + \sqrt{165} L_{11} \bar{I}(1, 4) + L_{20} \bar{I}(0, 5) \right) \\
\bar{I}(1, 6) &= \bar{L}_{16} - \frac{351\sqrt{65}}{40} \bar{L}_{12} - \frac{11\sqrt{13}}{2} \bar{I}(1, 4) - \frac{1}{L_{00}} \left(\frac{45\sqrt{13}}{2} \bar{L}_{02} \bar{L}_{12} + \frac{11\sqrt{65}}{5} \bar{L}_{04} \bar{L}_{12} \right. \\
&\quad \left. + \frac{109\sqrt{273}}{30} \bar{L}_{11} \bar{L}_{03} + \frac{33\sqrt{13}}{5} \bar{L}_{13} \bar{L}_{03} + \frac{11\sqrt{65}}{5} \bar{L}_{02} \bar{I}(1, 4) + \frac{\sqrt{429}}{3} \bar{L}_{11} \bar{I}(0, 5) \right) \\
\bar{I}(0, 7) &= L_{07} - \frac{1727\sqrt{105}}{120} L_{03} - \frac{13\sqrt{165}}{6} \bar{I}(0, 5) \\
&\quad - \frac{1}{L_{00}} \left(\frac{1595\sqrt{21}}{42} L_{02} L_{03} + \frac{143\sqrt{105}}{35} L_{04} L_{03} + \frac{13\sqrt{33}}{3} L_{02} \bar{I}(0, 5) \right)
\end{aligned}$$

References:

- 1 . Campisi P , Egiazarian K . Blind image deconvolution: Theory and Applications . CRC Press ; 2007 ;
- 2 . Savakis A , Trussell HJ . Blur identification by residual spectral matching . IEEE Trans Image Process . 2 : (2) 141 - 151 1993 ;
- 3 . Molina R , Mateos J , Katsaggelos AK . Blind deconvolution using a variational approach to parameter, image, and blur estimation . IEEE Trans Image Process . 15 : (12) 3715 - 3727 2006 ;
- 4 . Sorel M , Flusser J . Space-variant restoration of images degraded by camera motion blur . IEEE Trans Image Process . 17 : (2) 105 - 116 2008 ;
- 5 . Jung SW , Kim TH , Ko SJ . A novel multiple image deblurring technique using fuzzy projection onto convex sets . IEEE Signal Process Lett . 16 : (3) 192 - 195 2009 ;
- 6 . Flusser J , Suk T , Saic S . Recognition of blurred images by the method of moments . IEEE Trans Image Process . 5 : (3) 533 - 538 1996 ;
- 7 . Flusser J , Suk T . Degraded image analysis: an invariant approach . IEEE Trans Pattern Anal Mach Intell . 20 : (6) 590 - 603 1998 ;
- 8 . Liu J , Zhang TX . Recognition of the blurred image by complex moment invariants . Pattern Recognition Lett . 26 : (8) 1128 - 1138 2005 ;
- 9 . Flusser J , Suk T , Saic S . Recognition of images degraded by linear motion blur without restoration . Comput Suppl . 11 : 37 - 51 1996 ;

- 10. Stern A , Kruchakov I , Yoavi E , Kopeika S . Recognition of motion-blurred images by use of the method of moments . Appl Opt . 41 : (11) 2164 - 2172 2002 ;
- 11 . Lu J , Yoshida Y . Blurred image recognition based on phase invariants . IEICE Trans Fundam Electron Comm Comput Sci . E82A : 1450 - 1455 1999 ;
- 12 . Wang XH , Zhao RC . Pattern recognition by combined invariants . Chin J Electron . 10 : (4) 480 - 483 2001 ;
- 13 . Zhang Y , Wen C , Zhang Y . Estimation of motion parameters from blurred images . Pattern Recognition Lett . 21 : (5) 425 - 433 2000 ;
- 14 . Zhang Y , Wen C , Zhang Y , Soh YC . Determination of blur and affine combined invariants by normalization . Pattern Recognit . 35 : (1) 211 - 221 2002 ;
- 15 . Zhang Y , Zhang Y , Wen C . A new focus measure method using moments . Image Vis Computing . 18 : (12) 959 - 965 2000 ;
- 16 . Flusser J , Zitova B . Combined invariants to linear filtering and rotation . Int J Pattern Recognition Artif Intell . 13 : (8) 1123 - 1136 1999 ;
- 17 . Flusser J , Zitova B , Suk T . Editor: Tammy IS . Invariant-based registration of rotated and blurred images . Proc. of the IEEE International Geoscience and Remote Sensing Symposium IGARSS'99 Hamburg, Germany 1262 - 1264 June 1999 ;
- 18 . Zitova B , Flusser J . Estimation of camera planar motion from defocused images . Proc. of the IEEE International Conference on Image Processing ICIP'02, vol. II Rochester, NY 329 - 332 September 2002 ;
- 19 . Suk T , Flusser J . Combined blur and affine moment invariants and their use in pattern recognition . Pattern Recognit . 36 : (12) 2895 - 2907 2003 ;
- 20 . Flusser J , Boldys J , Zitova B . Moment forms invariant to rotation and blur in arbitrary number of dimensions . IEEE Trans Pattern Anal Mach Intel . 25 : (2) 234 - 246 2003 ;
- 21 . Candocia FM . Moment relations and blur invariant conditions for finite-extent signals in one, two and N-dimensions . Pattern Recognit Lett . 25 : (4) 437 - 447 2004 ;
- 22 . Teague M . Image analysis via the general theory of moments . J Opt Soc Am . 70 : (8) 920 - 930 1980 ;
- 23 . Teh CH , Chin RT . On image analysis by the method of moments . IEEE Trans Pattern Anal Mach Intel . 10 : (4) 496 - 513 1988 ;
- 24 . Shu HZ , Luo LM , Coatrieux JL . Moment-based approaches in image Part 1: basic features . IEEE Eng Med Biol Mag . 26 : (5) 70 - 75 2007 ;
- 25 . Shu HZ , Luo LM , Coatrieux JL . Moment-based approaches in image Part 2: invariance . IEEE Eng Med Biol Mag . 27 : (1) 81 - 83 2008 ;
- 26 . Shu HZ , Luo LM , Coatrieux JL . Moment-based approaches in image Part 3: computational considerations . IEEE Eng Med Biol Mag . 27 : (3) 89 - 91 2008 ;
- 27 . Shu HZ , Luo LM , Coatrieux JL . Moment-based approaches in imaging Part 4: some applications . IEEE Eng Med Biol Mag . 27 : (5) 116 - 118 2008 ;
- 28 . Mukundan R , Ramakrishnan KR . Moment Functions in Image Analysis—Theory and Applications . World Scientific ; Singapore 1998 ;
- 29 . Shu HZ , Zhou J , Han GN , Luo LM , Coatrieux JL . Image reconstruction from limited range projections using orthogonal moments . Pattern Recognit . 40 : (2) 670 - 680 2007 ;
- 30 . <http://www1.cs.columbia.edu/CAVE/software/softlib/coil-20.php>

Fig. 1

The standard gray-level image of cat with size 128×128



Fig. 2

Some examples of the blurred image: (a) averaging blur with additive zero-mean Gaussian noise, STD=10; (b) motion blur with additive zero-mean Gaussian noise, STD = 20; (c) out-of-focus blur with additive salt-and-pepper noise, density = 0.01, (d) Gaussian blur with additive salt-and-pepper noise, density = 0.02.

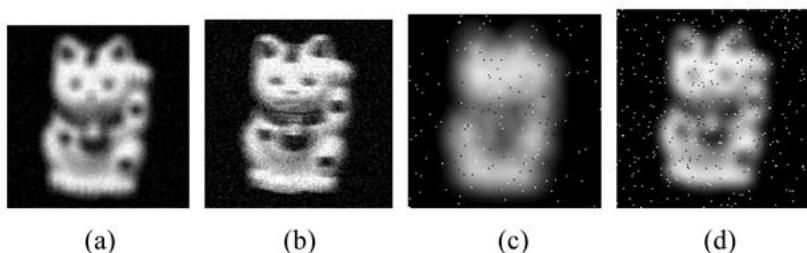


Fig. 3

Relative error for averaging blur with Gaussian noise shown in Fig. 2(a) . Horizontal axis: standard deviation of noise; vertical axis: relative error between the corrupted image and original image.

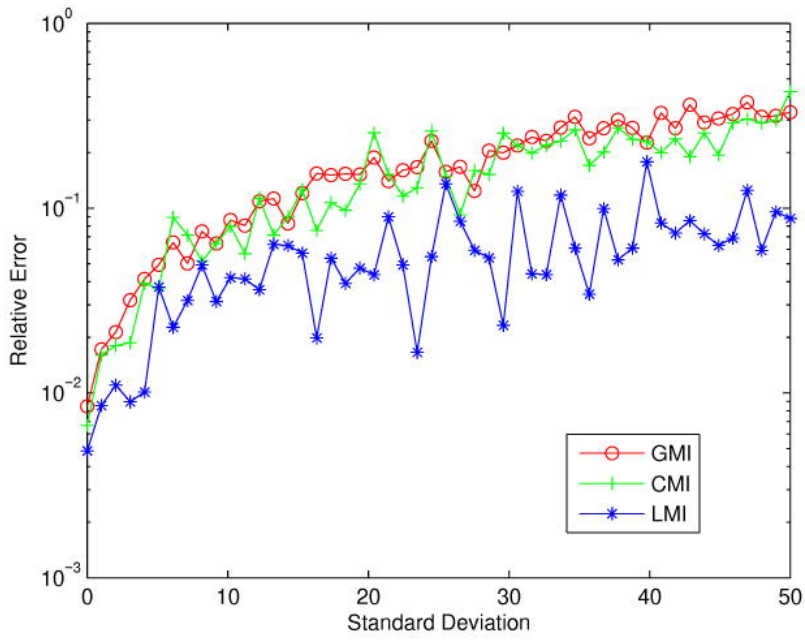


Fig. 4

Relative error for motion blur with Gaussian noise shown in Fig. 2(b) . Horizontal axis: standard deviation of noise; vertical axis: relative error between the corrupted image and original image.

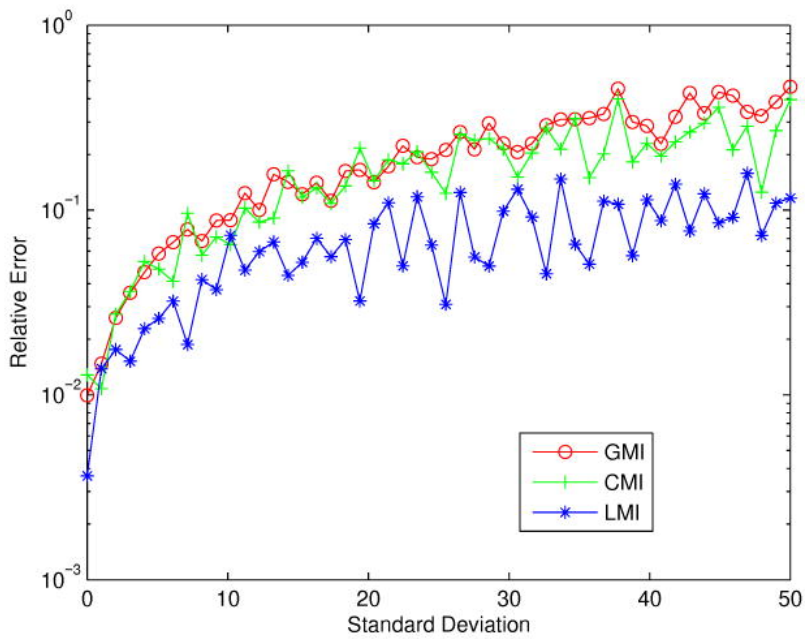


Fig. 5

Relative error for out-of-focus blur with salt-and-pepper noise shown in Fig. 2(c) . Horizontal axis: noise density; vertical axis: relative error between the corrupted image and original image.

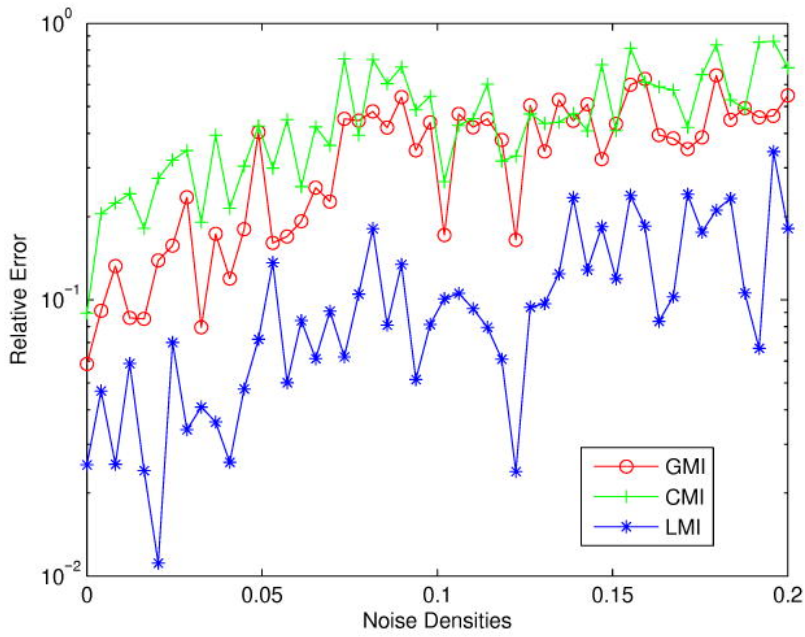


Fig. 6

Relative error for Gaussian blur adding salt-and-pepper noise shown in Fig. 2(d) . Horizontal axis: noise density; vertical axis: relative error between the corrupted image and original image.

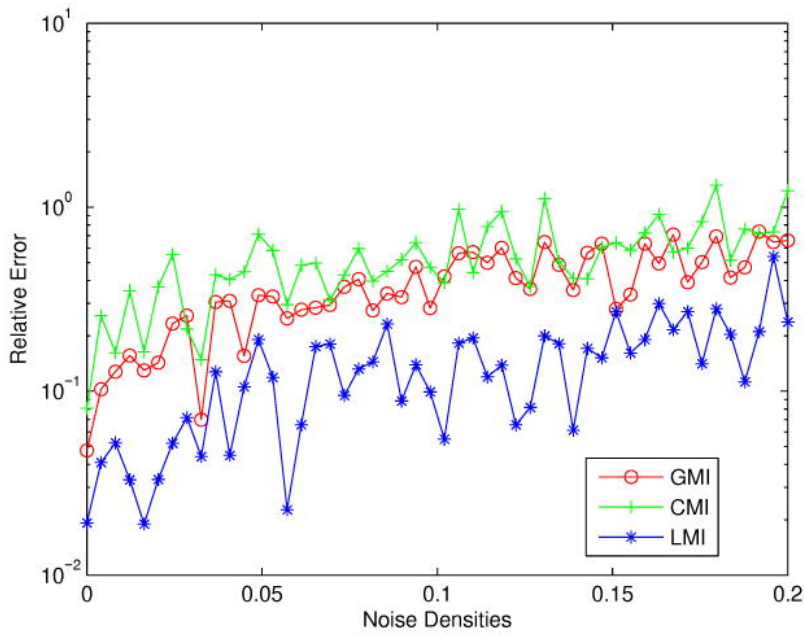


Fig. 7

Original images of alphanumeric characters for invariant character recognition



Fig. 8

Eight objects selected from the Coil-100 image database of Columbia University

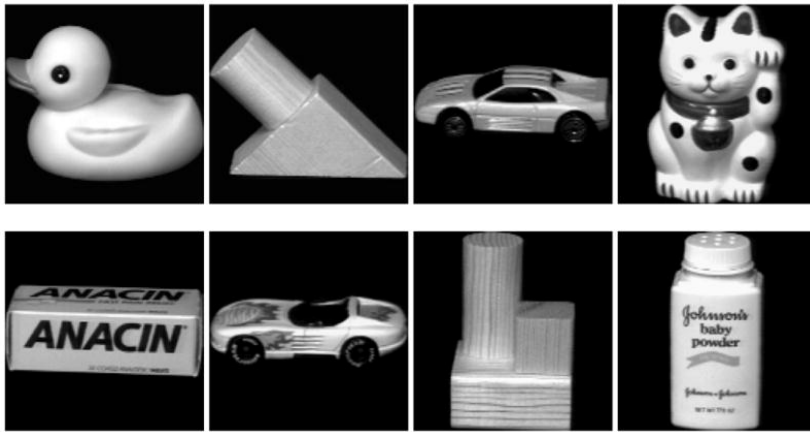


Fig. 9

Some examples of the blurred images corrupted by various types of noise

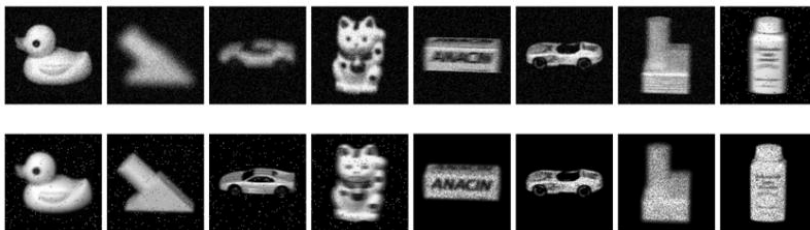


Fig. 10

The comb. The extent of out-of-focus blur increases from Image1 to Image8.

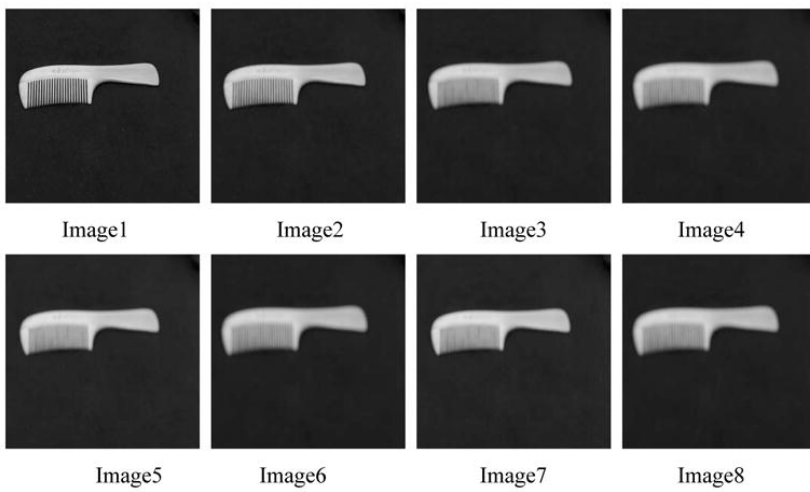


Table 1

The recognition rates obtained respectively with GMI, CMI and LMI for alphanumeric character in Fig. 7

	GMI	CMI	LMI
Noise-free	100%	100%	100%
Additive white noise with STD=1	92.08%	91.88%	100%
Additive white noise with STD=3	85%	82.92%	97.71%
Additive white noise with STD=5	77.29%	75.42%	90%
Additive salt-and-pepper noise with noise density = 0.2%	91.04%	87.08%	97.92%
Additive salt-and-pepper noise with noise density = 0.4%	83.75%	83.54%	94.79%
Additive salt-and-pepper noise with noise density = 0.8%	77.33%	75.67%	90%
Additive multiplicative noise with noise density = 0.01	95.83%	90.63%	98.13%
Additive multiplicative noise with noise density = 0.03	95%	86.88%	97.5%
Additive multiplicative noise with noise density = 0.05	91.25%	85.21%	95%
Computation time	6.86s	27.08s	6.95s

Table 2

The recognition rates of the GMI, CMI and LMI in object recognition (Fig. 9)

	GMI	CMI	LMI
Noise-free	100%	100%	100%
Additive white noise with STD=8	78.33%	80%	96.25%
Additive white noise with STD=16	68.96%	62.71%	83.96%
Additive white noise with STD=25	60.42%	50.62%	74.79%
Additive salt-and-pepper noise with noise density = 0.01	87.29%	76.46%	97.08%
Additive salt-and-pepper noise with noise density = 0.02	73.33%	64.38%	85.83%
Additive salt-and-pepper noise with noise density = 0.03	68.13%	56.46%	79.37%
Additive multiplicative noise with noise density = 0.1	100%	99.17%	100%
Additive multiplicative noise with noise density = 0.3	96.25%	87.92%	99.38%
Additive multiplicative noise with noise density = 0.5	90%	81.88%	95.63%
Computation time	9.42s	44.14s	9.80s

Table 3

GMI CMI and LMI values of the real images in Fig. 10

	Image1	Image2	Image3	Image4	Image5	Image6	Image7	Image8	σ / μ
G (5, 0)	-0.328	-0.319	-0.324	-0.322	-0.324	-0.329	-0.357	-0.363	5.07%
C (5, 0)	35.01	34.95	34.51	34.34	34.38	34.44	40.28	40.62	7.54%
L (5, 0)	-66.3	-66.3	-68.2	-68.5	-69.1	-69.9	-71.9	-72.8	3.42%
G (4, 1)	-0.0622	-0.0658	-0.0671	-0.0669	-0.0669	-0.0674	-0.0720	-0.0725	4.91%
C (4, 1)	50.20	50.02	49.40	49.18	49.21	49.33	57.61	58.15	7.5%
L (4, 1)	-11.4	-12.4	-12.8	-12.9	-13.0	-13.0	-13.1	-13.2	4.62%
G (3, 2)	-0.0190	-0.0179	-0.0174	-0.0165	-0.0166	-0.0169	-0.0219	-0.0222	12.43%
C (3, 2)	60.14	59.86	59.13	58.88	58.90	59.07	68.92	69.59	7.47%
L (3, 2)	-12.9	-13.0	-13.4	-13.4	-13.5	-13.7	-14.2	-14.3	3.72%
G (2, 3)	-0.0262	-0.0278	-0.0278	-0.0274	-0.0273	-0.0274	-0.0313	-0.0316	6.98%
C (2, 3)	60.14	59.86	59.13	58.88	58.90	59.07	68.92	69.59	7.47%
L (2, 3)	-10.6	-11.7	-12.1	-12.2	-12.2	-12.2	-12.5	-12.5	5.16%
G (1, 4)	-0.0485	-0.0479	-0.0480	-0.0468	-0.0471	-0.0475	-0.0549	-0.0554	7.11%
C (1, 4)	50.20	50.02	49.40	49.18	49.21	49.33	57.61	58.15	7.5%
L (1, 4)	-8.84	-8.79	-8.89	-8.72	-8.79	-8.86	-9.98	-10.06	6.15%
G (0, 5)	-0.223	-0.250	-0.257	-0.257	-0.257	-0.258	-0.269	-0.269	5.67%
C (0, 5)	35.01	34.95	34.51	34.34	34.38	34.44	40.28	40.62	7.54%
L (0, 5)	-40.6	-45.4	-46.8	-46.8	-46.9	-47.1	-48.6	-48.6	5.49%